

From Cavitation to Astrophysics: Explicit Solution of the Spherical Collapse Equation

Danail Obreschkow

*International Centre for Radio Astronomy Research, M468,
University of Western Australia, 35 Stirling Hwy, Perth, WA 6009, Australia*

(Dated: March 20, 2024)

Differential equations of the form $\ddot{R} = -kR^\gamma$, with a positive constant k and real parameter γ , are fundamental in describing phenomena such as the spherical gravitational collapse ($\gamma = -2$), the implosion of cavitation bubbles ($\gamma = -4$) and the orbital decay in binary black holes ($\gamma = -7$). While explicit elemental solutions exist for select integer values of γ , more comprehensive solutions encompassing larger subsets of γ have been independently developed in hydrostatics (see Lane-Emden equation) and hydrodynamics (see Rayleigh-Plesset equation). I here present a universal explicit solution for all real γ , invoking the beta distribution. Although standard numerical ODE solvers can readily evaluate more general second order differential equations, this explicit solution reveals a hidden connection between collapse motions and probability theory that enables further analytical manipulations, it conceptually unifies distinct fields, and it offers insights into symmetry properties, thereby enhancing our understanding of these pervasive differential equations.

I. INTRODUCTION

It may be surprising that the 21st century still holds critically important differential equations, which admit compact, but barely known explicit solutions. In this paper, I discuss such a family of equations that govern all physical systems described by a one-dimensional time-dependent coordinate $R(T)$, subject to a restoring force that varies as a power law of that coordinate. Formally, this is expressed by the non-linear ordinary differential equation (ODE)

$$\ddot{R} = -kR^\gamma \quad (1)$$

with fixed $k \in \mathbb{R}_+$ and $\gamma \in \mathbb{R}$. Dots denote derivatives with respect to time T . Using a capital T , normally reserved for temperature, will help distinguish this time from a dimensionless time t (Section II A). We may call Equation (1) the ‘spherical collapse equation’ by virtue of its most common applications.

I will restrict the discussion to the case, where R exhibits a finite maximum R_0 —in many physical applications this is equivalent to stating that the system is ‘bound’. Equation (1) being an autonomous ODE, we can always choose the origin of time to coincide with $R = R_0$, in which case the initial conditions read

$$R(0) = R_0 \quad \text{and} \quad \dot{R}(0) = 0. \quad (2)$$

Equations (1) and (2) are manifestly time-symmetric, i.e., $R(T) = R(-T)$ where a solution exists. Often most relevant is the time interval $T \in [0, T_c]$, from the maximum radius to the (first) collapse point, $R(T_c) = 0$. I will focus on this interval for most of this paper.

Table I lists textbook examples of physical systems governed by Equation (1). Many of them are encountered at undergraduate levels and used to illustrate cases, whose solution $R(T)$ must be obtained via numerical ODE solvers, such as Runge–Kutta solvers. The existence, let alone the form, of an explicit solution is rarely

noted, except, of course, in trivial cases like the linear free-fall ($\gamma = 0$) and harmonic oscillator ($\gamma = 1$).

An iconic example of Equation (1) in astrophysics is the gravitational collapse of a uniform collisionless sphere ($\gamma = -2$), the so-called top-hat spherical collapse model [1]. A simple parametric solution, $\{T(\theta), R(\theta)\}$ [2], has become the default solution in cosmology. Its transcendental nature implies that algebraic solutions of Equation (1) do not generally exist, yet the search for non-algebraic [3] and approximate [4] solutions continues.

Barely known to astrophysicists, an analogous collapse equation (but with $\gamma = -4$) has long been studied in hydrodynamics [5]. This equation, named after Lord Rayleigh [6], describes the collapse of an empty spherical cavity in an ideal incompressible liquid. Recent approximations [7] have led to the development of an infinite series that rapidly converges toward the exact solution [8]. Shortly after, others presented the first closed-form solution for cavities in three [9] and $N \geq 3$ [10] dimensions, in terms of hypergeometric functions.

Equation (1) is also encountered in static systems. For example, it is equivalent to the one-dimensional Lane-Emden equation [11, 12], describing the density profile of a self-gravitating polytropic gas in a thin tube in hydrostatic equilibrium. A classic solution for $\gamma > -1$ has been found in the context of galactic discs [13].

Building on the special solutions found independently in different fields, this paper presents a compact general explicit solution of Equation (1). While overall straightforward, the path to this solution involves some subtleties that enable the generalisation to all real γ . This allows us to discuss various seemingly unrelated basic problems in physics and astrophysics in unison. Section II overviews reformulations, useful for the derivation of the general solution in Section III and its discussion in Section IV. Section V concludes with a brief synthesis and outlook.

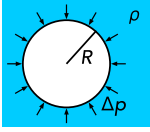
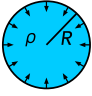
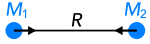
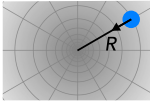
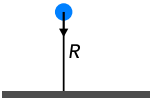
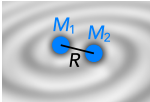
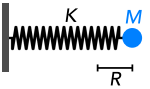
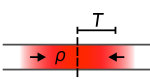
Physical system	Schematic	Meaning of R	Time scale T_0	γ	τ
Cavitation bubble Spherical cavity of constant (possibly zero) internal pressure, imploding under the pressure of an incompressible inviscid liquid without surface tension		Bubble radius	$R_0 \sqrt{\rho/\Delta p}$, where ρ is the density of the liquid and $\Delta p = p_\infty - p_v$, with far-field liquid pressure p_∞ and constant bubble pressure p_v	-4	≈ 0.91468
Generalisation to a spherical bubble in $N \geq 3$ dimensions [e.g., 14]			$(N - 2)^{-1/2} R_0 \sqrt{\rho/\Delta p}$	$-N - 1$	(Eq. 16)
Gravitational collapse Collapse of a uniform sphere, also known as spherical top-hat, subjected only to gravitational forces		Radius of sphere	$\sqrt{3/(4\pi G \rho_0)}$, where ρ_0 is the initial density at the onset of the collapse and G is the gravitational constant	-2	$\pi/\sqrt{8} \approx 1.11072$
Two-body collision Two point masses in gravitational free-fall toward each other, on a straight line without angular momentum		Distance between the centres of the two masses	$R_0^{3/2}/\sqrt{G(M_1 + M_2)}$, where M_i denote the two masses and G is the gravitational constant	-2	$\pi/\sqrt{8} \approx 1.11072$
Free-fall in spherical potential Radial free-fall in a spherically symmetric gravitational power law potential, $\phi \sim R^\alpha$, with index $\alpha \neq 0$		Distance from centre of potential	$\sqrt{(L/R_0)^\alpha/\alpha} \cdot R_0/V$, where L and V are the length and velocity scales of the potential $\phi(R) = \text{sgn}(\alpha) \cdot V^2 \cdot (R/L)^\alpha$	$\alpha - 1$	(Eq. 16)
Same for a logarithmic potential, e.g., the potential of a singular isothermal sphere			R_0/V , where V is the velocity scale in $\phi(R) = V^2 \ln(R/L)$	-1	$\sqrt{\pi/2} \approx 1.25331$
Free-fall in uniform field Straight fall in a constant acceleration field, such as a vertical drag-free drop of an object on Earth		Height from the ground	$\sqrt{R_0/g}$, where g is the norm of the constant acceleration, e.g., $g = 9.81\text{m s}^{-2}$ on Earth	0	$\sqrt{2} \approx 1.41421$
Relativistic orbital decay Orbital decay by gravitational radiation of two masses at non-relativistic velocities, initially forced on circular orbits		Distance between the centres of the two masses	$\frac{5c^5 R_0^4}{64\sqrt{3}G^3 M_1 M_2 (M_1 + M_2)}$, with M_i the two masses, G the gravitational constant and c the speed of light	-7	≈ 0.74683
Harmonic oscillator Motion of a mass attached to an ideal spring, initially at rest in an extended or compressed state		Distance from the equilibrium position	$\sqrt{M/K}$, where M is the mass and K the spring constant	+1	$\pi/2 \approx 1.57080$
Polytrope Density profile of a self-gravitating polytropic gas in one dimension in hydrostatic equilibrium		$\rho^{1/n}$, where ρ is the gas density and n the index of $p = K\rho^{1+1/n}$	$\sqrt{(1+n)KR_0^{1-n}/(4\pi G)}$ is a length scale set by the parameters of the polytropic equation of state $p = K\rho^{1+1/n}$	n	(Eq. 16)

TABLE I. Textbook examples of systems governed by Equations (1) and (2). Moving objects described by $R(T)$ are shown in blue, whereas static objects described by this equation are shown in red. T_0 is the characteristic physical scale (normally a characteristic time), such that Equation (1) reduces to the dimensionless Equation (5) upon normalisation via Equation (3). The collapse time is T_c , satisfying $R(T_c) = 0$, is given by $T_0\tau$. Where T_0 depends on R_0 , the latter is the maximum, initial value of R . In the case of the polytrope (bottom row), R and T have different meanings: $R := \rho^{1/n}$ is a measure of the gas density and T is the distance from the centre of mass. For most examples, analogous cases with other forces, such as electric forces instead of gravitational ones, can be found.

II. SETTING THE STAGE

Before delving into the solutions of Equation (1), it is worth recalling basic, but pivotal remarks on equivalent reformulations. These will help the derivation (Section III) and discussion (Section IV) of the solutions.

A. Dimensionless form

The first remark is that it is convenient to work in dimensionless position and time coordinates, defined as

$$r := \frac{R}{R_0} \quad \text{and} \quad t := \frac{T}{T_0}, \quad (3)$$

where $R_0 = R(0)$ is the maximum, initial value of R (c.f., Equation 2) and

$$T_0 := \sqrt{k^{-1}R_0^{1-\gamma}} \quad (4)$$

is the natural time constant. With this normalisation, Equation (1) becomes

$$\ddot{r} = -r^\gamma, \quad (5)$$

and the initial conditions (Equation 2) become

$$r(0) = 1 \quad \text{and} \quad \dot{r}(0) = 0. \quad (6)$$

It is understood that dots above $r(t)$ now denote derivatives with respect to t , rather than T . To help the following derivations, we introduce the variable $\tau := T_c/T_0$ as a shorthand for the dimensionless collapse time.

The constant k has conveniently disappeared in the dimensionless form of Equation (5), reducing the family of ODEs to a single control parameter γ . The natural disappearance of k brings to light the inherently scale-free nature of Equation (1) implied by its power law structure. This is the deeper reason for Equation (1) to be applicable from microscopic to astrophysical scales.

As a textbook example, let us consider the gravitational collapse of a uniform pressure-free sphere, initially at rest with radius $R(0) = R_0$. The Newtonian equation of motion reads

$$\frac{d^2 R}{dT^2} = -\frac{GM}{R^2}, \quad (7)$$

which is Equation (1) with $\gamma = -2$ and $k = GM$. Upon expressing R and T in their natural units R_0 and $T_0 = \sqrt{R_0^3/(GM)}$, Equation (7) becomes indeed $\ddot{r} = -r^{-2}$.

B. Equivalent formulations

The second remark is that Equation (5), and thus Equation (1), can be rewritten in other differential forms.

1. Integral of motion

Most importantly, Equation (5) always exhibits an *integral of motion*,

$$0 = \begin{cases} \frac{1+\gamma}{2}\dot{r}^2 + r^{1+\gamma} - 1 & \text{if } \gamma \neq -1 \\ \dot{r}^2 + 2 \ln r & \text{if } \gamma = -1 \end{cases} \quad (8a)$$

$$(8b)$$

If differentiated with respect to t and solved for \ddot{r} , Equation (8) becomes Equation (5), except if $\dot{r} = 0$. Since Equations (8) are first-order differential equations, only one boundary condition is required, such as $r(0) = 1$.

2. Hybrid differential equation

If $\gamma \neq -1$, a hybrid ODE, mixing first and second derivatives, can be obtained by rewriting $r^{1+\gamma}$ in Equation (8a) as $rr^\gamma = -r\ddot{r}$ (Equation 5), hence

$$1 - \frac{1+\gamma}{2}\dot{r}^2 + r\ddot{r} = 0. \quad (9)$$

This is, for example, the standard form of the equation describing the collapse of a spherical cavitation bubble without viscosity and surface tension [6], normally written in dimensional form,

$$\frac{3}{2} \left(\frac{dR}{dT} \right)^2 + R \frac{d^2 R}{dT^2} + \frac{\Delta p}{\rho} = 0, \quad (10)$$

where Δp is the driving pressure and ρ the constant liquid density (see first row in Table I). Expressed in natural units, $R_0 = R(0)$ and $T_0 = R_0 \sqrt{\rho/\Delta p}$, Equation (10) becomes Equation (9) with $\gamma = -4$. Thus Equation (10) is equivalent to Equation (1) with $\gamma = -4$ and $k = R_0^3 \Delta p / \rho$.

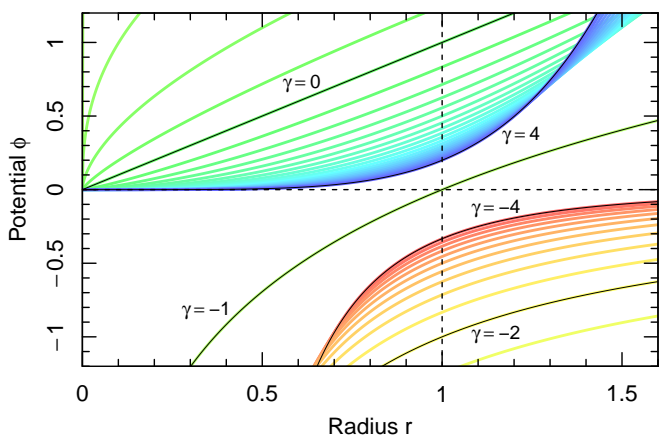


FIG. 1. Potential $\phi(r)$, given in Equation (12), for different values of γ , equally spaced by $\Delta\gamma = 0.2$. There are qualitatively distinct families at $\gamma < -1$ (red-yellow) and $\gamma > -1$ (blue-green), as discussed in Section IV A. They are separated by an isolated critical curve for $\gamma = -1$. Thin black lines highlight the coloured curves with a printed γ -value.

3. Lagrangian

Finally, with an eye on applications in physics, it is worth noting that Equation (5) derives from a time-independent Lagrangian

$$\mathcal{L}(r, \dot{r}) = \frac{\dot{r}^2}{2} - \phi(r) \quad (11)$$

with the potential, defined up to an additive constant,

$$\phi(r) = \begin{cases} r^{1+\gamma}/(1+\gamma) & \text{if } \gamma \neq -1 \\ \ln r & \text{if } \gamma = -1 \end{cases} \quad (12)$$

The Euler-Lagrange equation, $\frac{d}{dt}(\partial\mathcal{L}/\partial\dot{r}) = \partial\mathcal{L}/\partial r$, then generates Equation (5), for all γ .

Selected potentials $\phi(r)$ are shown in Figure 1. The existence of two regimes, separated by the critical value $\gamma = -1$, is the fundamental reason for the qualitatively different behaviour of $r(t)$ in these regimes. These regimes will be discussed in more detail in Section IV A.

III. GENERAL SOLUTION

In this section, I present compact general solutions of Equation (1) with initial conditions of Equation (2), following an approach similar to [9], but for general real parameters γ . For convenience, all derivations and solutions are presented for the dimensionless form in Equation (5) with initial conditions stated in Equation (6). Any solution $r(t)$ can be transformed to the corresponding dimensional solution $R(T)$ via the linear transformations of Equation (3).

A. Inverse solution $t(r)$

1. Cases $\gamma \neq -1$

This case can be solved by reduction to quadrature, a standard method expressing the solution of ODEs in terms of integrals. For general second order ODEs, $\ddot{f}(t) = f(\dot{r}, r, t)$, the integrals found in this way must be evaluated numerically. Interestingly, however, the limited form of Equation (5) allows us, through adequate substitutions, to express the emerging integrals through the *incomplete beta function* $B(x; \alpha, \beta)$ (derivation in Appendix A). This special function benefits from an extensive mathematical literature available for further analytical manipulations of the solution. Moreover, by introducing the shorthands

$$\eta = \frac{1}{|1+\gamma|}, \quad (13)$$

and

$$\alpha = \frac{1}{4} + \frac{3-\gamma}{4|1+\gamma|}, \quad (14)$$

it turns out possible to compact the explicit solution $r(t)$ to a universal form, valid for all $\gamma \neq -1$, hence simplifying and generalising state-of-the-art hypergeometric solutions for $\gamma = -4$ [9] and lower negative integer γ [10].

Explicitly, Equations (5) and (6) solve to

$$t(r) = \tau - \sqrt{\frac{\eta}{2}} B\left(r^{|1+\gamma|}; \alpha, \frac{1}{2}\right), \quad (15)$$

following the derivation provided in Appendix A. The collapse time τ is obtained by solving Equation (15) for τ at $(r, t) = (1, 0)$,

$$\tau(\gamma) = \sqrt{\frac{\eta}{2}} B\left(\alpha, \frac{1}{2}\right). \quad (16)$$

Here $B(\alpha, \beta)$ is the (complete) *beta function*, i.e., the incomplete $B(x; \alpha, \beta)$ evaluated at $x = 1$. Selected explicit values of τ are listed in Table II.

Substituting Equation (16) back into Equation (15), the latter can be transformed to the special solution for $\gamma > -1$ found in modelling polytropic gas densities in galactic disks [13].

2. Special case $\gamma = -1$

In this case, Equation (8b) integrates to

$$t(r) = \tau(-1) \operatorname{erf}\left(\sqrt{-\ln r}\right) \quad (17)$$

where

$$\tau(-1) = \sqrt{\pi/2} \quad (18)$$

is the collapse time, reached for $r \rightarrow 0_+$. This collapse time is equal to the limit of Equation (16) for $\gamma \rightarrow -1$. Likewise, Equation (17) is the limit of Equation (15) for $\gamma \rightarrow -1$, showing that these singularities of Equations (15) and (16) at $\gamma = -1$ are removable.

B. Explicit solution $r(t)$

To invert the solutions $t(r)$ it is convenient to normalise Equation (15) by τ , which yields

$$\frac{t}{\tau} = 1 - I\left(r^{|1+\gamma|}; \alpha, \frac{1}{2}\right), \quad (19)$$

where $I(x; \alpha, \beta) \equiv B(x; \alpha, \beta)/B(\alpha, \beta)$ is called the *regularised incomplete beta function* (a simple, but useful step pointed out by Roberto Iacono, priv. com.). Equations (19) and (17) can be readily inverted to a compact general explicit solution in terms of well-known special functions,

$$r(t) = \begin{cases} Q\left(1 - \frac{|t|}{\tau(\gamma)}; \alpha, \frac{1}{2}\right)^\eta & \text{if } \gamma \neq -1 \\ \exp\left(-\operatorname{erfi}^2\left(\sqrt{2/\pi} t\right)\right) & \text{if } \gamma = -1 \end{cases} \quad (20a)$$

$$(20b)$$

γ	τ (exact)	τ (num)	$\dot{r}(\tau)$ (exact)	$\dot{r}(\tau)$ (num)
$-\infty$	0	0	$-\infty$	$-\infty$
-100	—	0.22019512	$-\infty$	$-\infty$
-10	—	0.64597784	$-\infty$	$-\infty$
-4	—	0.91468136	$-\infty$	$-\infty$
-3	1	1	$-\infty$	$-\infty$
-2	$\pi/\sqrt{8}$	1.11072073	$-\infty$	$-\infty$
-5/3	$2/\sqrt{3}$	1.15470054	$-\infty$	$-\infty$
-3/2	$3\pi/8$	1.17809725	$-\infty$	$-\infty$
-4/3	$\pi\sqrt{75/512}$	1.20239047	$-\infty$	$-\infty$
-1	$\sqrt{\pi/2}$	1.25331414	$-\infty$	$-\infty$
-2/3	$\sqrt{128/75}$	1.30639453	$-\sqrt{6}$	-2.44948974
-1/2	4/3	1.33333333	-2	-2
-1/3	$\pi\sqrt{3}/4$	1.36034952	$-\sqrt{3}$	-1.73205081
0	$\sqrt{2}$	1.41421356	$-\sqrt{2}$	-1.41421356
1	$\pi/2$	1.57079633	-1	-1
2	—	1.71731534	$-\sqrt{2/3}$	-0.81649658
3	—	1.85407468	$-1/\sqrt{2}$	-0.70710678
4	—	1.98232217	$-\sqrt{2/5}$	-0.63245553
10	—	2.62843161	$-\sqrt{2/11}$	-0.42640143
100	—	7.20340190	$-\sqrt{2/101}$	-0.14071951
∞	∞	∞	0	0

TABLE II. List of dimensionless collapse times τ , given by Equations (16) and (18), and dimensionless collapse point velocities $\dot{r}(\tau)$, given by Equation (23). Exact solutions are given where they are algebraic, at least up to a factor π .

where $\text{erfi}(x)$ is the *inverse error function* and $Q(x; \alpha, \beta)$ is the *inverse regularised incomplete beta function*. Equation (20b) is the limit of Equation (20a) for $\gamma \rightarrow -1$, again showing that this singularity of Equation (20a) is of a removable type.

The absolute value $|t|$ in Equation (20a) does not follow from Equation (19), only valid for $t \in [0, \tau]$. It is an ad-hoc extension of $r(t)$ to the domain $t \in [-\tau, \tau]$, exploiting the time-reversal symmetry of Equations (5) and (6). Equation (20b) is already time-symmetric and hence valid on $t \in [-\tau, \tau]$.

The significance of Equation (20) relies in the fact that the regularised incomplete beta function $I(x; \alpha, \beta)$ is the cumulative density function of the *beta distribution*, a common distribution function in probability theory, related to, but not to be confused with, the beta function. Hence, the function $Q(x; \alpha, \beta)$ is the quantile function of the beta distribution. This connection to the beta distribution, which has been intensively studied in probability theory, makes Equation (20) a practical solution for further analytical manipulations. Moreover, the quantile function $Q(x; \alpha, \beta)$ is readily accessible to all modern programming languages, making this solution easy to implement. Two examples in PYTHON and R are given in Appendix B.

Figure 2 shows $r(t)$ on the interval $t \in [0, \tau(\gamma)]$ for all integer γ from -4 to $+4$. Key properties of these solutions will be discussed in Section IV.

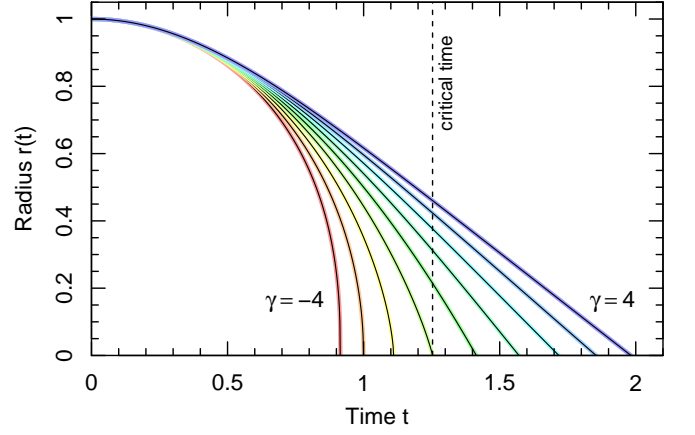


FIG. 2. Exact solutions of the normalised collapse Equation (5) with initial conditions of Equation (6), evaluated on $t \in [0, \tau(\gamma)]$ using the explicit Equation (20). Coloured curves correspond to different values of γ , separated by $\Delta\gamma = 1$. The dashed vertical line marks the collapse time $\sqrt{\pi}/2$, corresponding to the critical exponent $\gamma = -1$ that separates the divergent behaviour of $\dot{r}(\tau)$ from the convergent one.

C. Noteworthy special solutions

For completeness, I note that for select values of γ , Equation (20a) can be reduced to well-known more compact solutions,

$$r(t) = \begin{cases} \sqrt{1-t^2} & \text{if } \gamma = -3 & (21a) \\ 1-t^2/2 & \text{if } \gamma = 0 & (21b) \\ \cos(t) & \text{if } \gamma = 1 & (21c) \\ \text{cn}(t, \frac{1}{2}) & \text{if } \gamma = 3, & (21d) \end{cases}$$

where $\text{cn}(x, y)$ is the Jacobi elliptic cosine function.

To my knowledge, Equations (21a–c) are the only explicit closed-form solutions, i.e., solutions in terms of commonly accepted basic functions. These three functions respectively describe an arc of a circle (Equation 21a), a parabola (Equation 21b), and a harmonic oscillation (Equation 21c). Textbook examples for the latter two are given in Table I.

Equation (21d) is a special case of the undamped and unforced Duffing equation [15], for which general solutions in terms of the Jacobi elliptic family have recently been derived [16].

For some other values of γ , parametric solutions have been found well before explicit solutions. A famous example is the case of $\gamma = -2$, describing, e.g., the spherical gravitational collapse (see Table I). In this case [2],

$$t = \frac{\theta + \sin \theta}{\sqrt{8}}, \quad r = \frac{1 + \cos \theta}{2}. \quad (22)$$

Varying θ from 0 to π generates the collapse phase, whereas varying it from $-\pi$ to 0 generates the symmetric growth phase. More lengthy parametric solutions have also been presented for other non-trivial cases, such as empty spherical cavitation bubbles ($\gamma = -4$) [17].

IV. DISCUSSION

The general solution of Equations (5) and (6) given by Equation (20) warrants a brief discussion. As a preliminary remark, the linear transformation (Equation 3) between the normalised form $r(t)$ and its dimensional analogue $R(T)$ makes it straightforward to apply all properties of $r(t)$ to $R(t)$, and vice versa. For instance, as mentioned in Section I, any solution of Equations (1) and (2) is invariant under time reversal. This symmetry equally applies to dimensionless coordinates, i.e., $r(t) = r(-t)$, for all t , where a solution $r(t)$ exists. For efficiency, I will therefore limit the discussion in this section to the normalised form $r(t)$ and to positive times.

A. Behaviour at collapse point

As illustrated in Figure 2, the steepness of the function $r(t)$ monotonically increases as the time sweeps from $t = 0$ ($r = 1$) to the collapse time $t = \tau$ ($r = 0$). Equation (8) shows this immediately and reveals that in the limit $t \rightarrow \tau_-$, the velocity \dot{r} becomes

$$\dot{r}(\tau) = \begin{cases} -\sqrt{2/(1+\gamma)} & \text{if } \gamma > -1 \\ -\infty & \text{if } \gamma \leq -1 \end{cases} . \quad (23)$$

Some explicit values of $\dot{r}(\tau)$ are listed in Table II.

The divergent behaviour of $\dot{r}(\tau)$ for $\gamma \leq -1$, which can often be interpreted as a positively diverging kinetic energy ($\propto \dot{r}^2$), is mimicked by a negatively diverging potential $\phi(r)$. In fact, following Equation (12),

$$\lim_{r \rightarrow 0^+} \phi(r) = \begin{cases} 0 & \text{if } \gamma > -1 \\ -\infty & \text{if } \gamma \leq -1 \end{cases} , \quad (24)$$

as is apparent in Figure 1.

Equations (23) and (24) highlight the existence of two distinct regimes in the domain $\gamma \in \mathbb{R}$, separated by the critical value $\gamma = -1$. This value corresponds to the only singularity of Equation (20a), which is removed by Equation (20b). The dimensionless collapse time for $\gamma = -1$ is exactly $\sqrt{\pi}/2$ (Equation 18), the value shown by the dashed vertical line in Figure 2. Following Equation (23), all curves reaching $r = 0$ to the left of this line do so vertically, whereas those to the right of the line come down at a finite slope.

The two regimes separated by $\gamma = -1$ correspond to different classes of physical problems (c.f., Table I), explaining why—to my knowledge—they have never been addressed simultaneously in previous literature.

The regime $\gamma < -1$, sometimes including $\gamma = -1$, often describes a spherical collapse—gravitational or hydrodynamic in nature (see Table I). In this case, the collapse motion $r(t)$ near $t = \tau$, is sometimes referred to as ‘violent collapse’ or ‘catastrophic collapse’. This description is quite literal, a saddening example being the implosion of the Titan submersible near the wreck of the

Titanic in the North Atlantic Ocean (18 June 2023). This implosion was likely approximated by Equation (1) with $\gamma = -4$, predicting a collapse time $T_c \approx 5$ ms, based on a capsule radius $R_0 \approx 1$ m, a driving pressure $\Delta p \approx 350$ bar and a water density $\rho \approx 10^3 \text{ kg m}^{-3}$.

The infinite velocity at the collapse point for $\gamma \leq -1$ is unphysical, as all real-world systems modelled by Equation (1) start deviating from this model near the collapse point. Secondary mechanisms, which might have been negligible for most of the collapse motion, suddenly become dominant, preventing the singularity. For example, in the case of collapsing cavitation bubbles, these mechanisms include shock waves (liquid compressibility), sonoluminescence, sonochemistry, vapour compression and micro-jetting [18]. In the case of matter collapsing by self-gravity, the mechanisms preventing the divergence could be asymmetries, smoothing the collapse point, and pressure forces, possibly enhanced by strong radiation and phase transitions, e.g., to a neutron star. If these mechanisms cannot prevent $\dot{R}(T)$ from approaching the speed of light, general relativistic effects take over, transforming the collapsing mass into a static black hole [19]. This is likely the fate of the cores of massive stars ($\gtrsim 25 M_\odot$) [20] and possibly also primordial gas clouds ($\sim 10^5 M_\odot$), collapsing directly into black holes [21].

B. Continuation past collapse point

The solution of Equation (20) is valid only on the interval $t \in [-\tau, \tau]$. However, Equation (5) integrates smoothly past the collapse point $t = \tau$, to negative values of r , if $\gamma \in \mathbb{N}_0$.

For non-negative even γ , the sign of \ddot{r} remains negative as $r < 0$. Hence the ‘collapse’ motion continues through the point $t = \tau$ with ever increasing velocity, such that $\lim_{t \rightarrow \infty} \dot{r} = -\infty$. The simplest example would be an object dropped to the ground (defined as $R = 0$) into a vertical shaft ($R < 0$) with constant acceleration g ($\gamma = 0$, see Table I).

For positive odd γ , however, $r(t)$ passes through $r(\tau) = 0$, while inverting the sign of \ddot{r} . Symmetry considerations imply that $r(t)$ then describes an oscillating curve of wavelength $\lambda = 4\tau$, made of reflections of the arc $r(t \in [0, \tau])$. This curve satisfies $r(0) = 1$, $r(\tau) = 0$, $r(2\tau) = -1$, $r(3\tau) = 0$, $r(4\tau) = 1$, and so forth. For $\gamma = 1$, the oscillation is harmonic (Equation 21c), for all larger odd γ , it is anharmonic (e.g., Equation 21d).

Non-integer positive γ generally lead to complex solutions $r(t) \in \mathbb{C}$, if integrated past the collapse point. In fact, immediately past this point, the acceleration has the complex argument $\arg(\ddot{r}) = (\gamma + 1)\pi$, implying that its imaginary part only vanishes for integer γ .

For negative γ , Equation (20) diverges as $r \rightarrow 0$. This is a coordinate singularity, which can, in principle, be removed through regularisation techniques, such 2-body and N -body regularisation in astrophysical gravitational simulations [22].

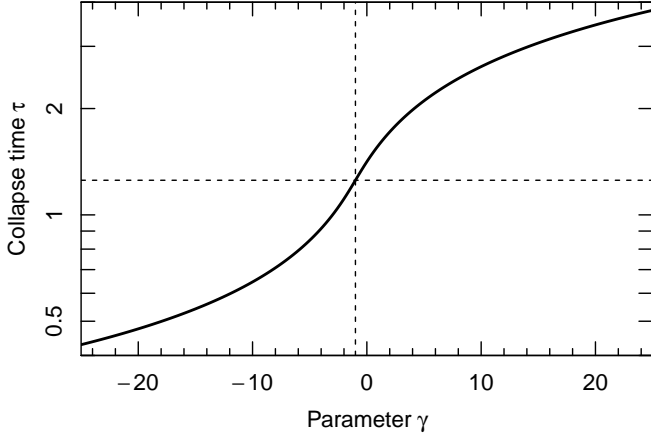


FIG. 3. Dimensionless collapse time $\tau = T_c/T_0$ as a function of the control parameter γ . Plotted in semi-log coordinates, this function exhibits a non-trivial point symmetry about $(\gamma = -1, \tau = \sqrt{\pi/2})$, marked by the dashed lines. See Section IV C.

C. Collapse time symmetry

Figure 3 shows the dimensionless collapse time τ as a function of the control parameter γ . With τ on a logarithmic axis, this function becomes a symmetric S-shape, which owes its symmetry to the beta function identity $B(\alpha, \beta)B(\alpha + \beta, 1 - \beta) = \pi/(\alpha \sin(\pi\beta))$. Applied to Equation (16), this identity implies that any point $(\gamma, \tau(\gamma))$ can be mapped onto a corresponding point

$$(\gamma, \tau) \mapsto \left(\gamma' = -2 - \gamma, \tau' = \frac{\pi}{2\tau} \right), \quad (25)$$

which also lies on the function $\tau(\gamma)$. This mapping is symmetric under the exchange of primed and non-primed variables. The only invariant point of this symmetry transformation, $\gamma = \gamma' = -1$ and $\tau = \tau' = \sqrt{\pi/2}$, is marked by the dashed lines in Figure 3. This point coincides with the special case of Equation (18), the singularity of Equation (20a) and the transition of $\dot{r}(\tau)$ from a finite to a diverging value (Section IV A).

D. General symmetry

A noteworthy property of Equation (5) is its formal invariance under a substitution $r \mapsto r' := r^\delta$, if $\delta = (1 - \gamma)/2$, provable by invoking Equation (9). The restriction to collapse motions, implying $r, r' \leq 1$ and $\ddot{r}, \ddot{r}' < 0$, limits the applicability of this substitution to positive δ , i.e., to $\gamma < 1$. A few elementary steps show that this substitution corresponds to the transformation

$$(\gamma, t, r) \mapsto \left(\gamma' = \frac{\gamma + 3}{\gamma - 1}, t' = t\sqrt{\frac{1 - \gamma}{2}}, r' = r^{\frac{1 - \gamma}{2}} \right). \quad (26)$$

Like Equation (25), this mapping is symmetric under the exchange of primed and non-primed variables; and like-

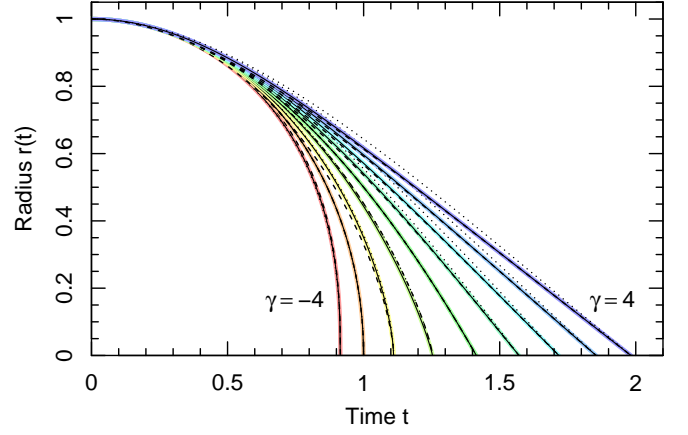


FIG. 4. Exact versus approximate solutions of the normalised collapse equation Equation (5) with initial conditions of Equation (6), evaluated on the normalised time interval $t \in [0, \tau(\gamma)]$. The selected values of γ are the same as in Figure 2. Solid lines are the exact solutions given in Equation (20), whereas dashed and dotted lines use the approximation of Equation (28) with parameters p_1 and q_1 (dashed) and p_2 and q_2 (dotted).

wise this symmetry transformation exhibits a single invariant point at $\gamma = \gamma' = -1$, where $(r', t') = (r, t)$.

The symmetry of Equation (25) can help identify new solutions based on existing ones, with the most trivial example being the derivation of Equation (21a) from Equation (21b), and vice versa.

When applying Equation (26) to dimensional quantities R and T instead of r and t , the physical constant k (Equation 1) must also be transformed, as $k' = k\delta R_0^{1+\gamma}$. For example, Rayleigh's Equation (10) can be written as

$$\frac{d^2 Z}{dt^2} = -\frac{5\Delta p}{2\rho} Z^{1/5}, \quad (27)$$

where $Z := R^{5/2}$.

E. Polynomial approximations

In some practical cases, it may be useful and sufficient to substitute the exact solution $r(t)$ given in Equation (20) by simple approximations $\tilde{r}(t)$. A possible choice is

$$\tilde{r}(t) = \begin{cases} (1 - x^2)^p & \text{if } \gamma \leq -1 \\ q(1 - |x|) - (q - 1)(1 - |x|)^{\frac{q}{q-1}} & \text{if } \gamma > -1, \end{cases} \quad (28a)$$

$$(28b)$$

where $x = t/\tau$ (with τ given in Equations (16) and (18)) and where $p \in (0, 1)$ and $q > 1$ are shape parameters.

These are arguably the simplest polynomials, which simultaneously satisfy six essential properties of the exact solution: (1) time symmetry, $\tilde{r}(t) = \tilde{r}(-t)$ if $t \in [-\tau, \tau]$; (2) negative curvature $\ddot{\tilde{r}}(t) < 0$ if $t \in (-\tau, \tau)$; (3) $\tilde{r}(0) = 1$; (4) $\tilde{r}(\tau) = 0$; (5) $\dot{\tilde{r}}(0) = 0$; and (6) $\lim_{t \rightarrow \tau} \dot{\tilde{r}}(t)$ is finite if and only if $\gamma > -1$.

Let us first consider Equation (28a) (case $\gamma \leq -1$), where the exponent p needs to be specified. Choosing p equal to $p_1 = 2/(1 - \gamma)$ (only for γ strictly below -1) ensures the correct asymptotic behaviour of \dot{r} as a function of \tilde{r} in the limit $t \rightarrow \tau$. Earlier, I introduced this approximation specifically for $\gamma = -4$ (thus $p = 2/5$) [7]. Equation (28a) can then be seen as the first term in a rapidly converging series, which tends toward the true solution if using exact analytical coefficients [8].

Alternatively, setting p equal to $p_2 = \tau^2/2$ (for all $\gamma \leq -1$), satisfies $\ddot{r}(0) = \dot{r}(0) = -1$. For $\gamma = -2$, the case of the gravitational collapse, this choice is $p = (\pi/4)^2 \approx 0.6169$. This is nearly identical to an analogous recent approximation [23], which reads $r(t) = (1 - t^2)^p$ with $p = 1.8614/3 \approx 0.6205$ determined via a fitting technique.

For Equation (28b) (case $\gamma > -1$), we have similar options for the parameter q . Setting it to $q_1 = \eta B(\eta, \frac{1}{2})$ (with η defined in Equation 13) ensures that $\dot{r}(\tau) = \dot{r}(\tau)$. Alternatively, setting it equal to $q_2 = \tau^2/(\tau^2 - 1)$ ensures $\ddot{r}(0) = \dot{r}(0) = -1$.

As shown in Figure 4, both of the above choices for p and q provide reasonable approximations of the exact solution. In general, the best pick depends on the application. If $\gamma = -3$ (hence $p_1 = p_2 = \frac{1}{2}$) or $\gamma = 0$ (hence $q_1 = q_2 = 2$), the two options are identical and Equations (28a) and (28b) become the exact solutions of Equations (21a) and (21b), respectively. Interestingly, these two solutions are related to each other via the symmetry transformation of Equation (26).

A more quantitative discussion of the approximations is beyond the scope of this paper, but can be found elsewhere for $\gamma = -4$ [7, 8].

V. CONCLUSION

This paper investigated the differential Equation (1) with boundary conditions stated in Equation (2). I have called this the spherical collapse equation in reference to its most common applications (c.f., Table I).

I have shown that this equation exhibits a unified explicit solution, invoking the beta distribution, a fundamental probability density function in statistics. Elements of the derivation can be found elsewhere, spread over decades of literature across several unrelated fields. The contribution of this work is to unify previously known parametric, implicit and explicit solutions from hydrodynamics (c.f., Rayleigh-Plesset equation), hydrostatics (Lane-Emden equation) and astrophysics (top-hat spherical collapse model), all limited to different subsets of γ , into a single concise solution (Equation 20a), universally valid for all real $\gamma \neq -1$. For $\gamma = -1$ this solution is singular, but its limit $\gamma \rightarrow -1$ exists, allowing the singularity to be removed via Equation (20b).

This general character ($\gamma \in \mathbb{R}$) of the explicit solution unifies seemingly unrelated physical applications. In this regard, this work provides context for recently found

apparent analogies between cavitation bubbles and processes in astronomy and cosmology [24–27].

The existence of a general explicit solution of Equation (1) is barely known, particularly in astrophysics and cosmology, where only parametric solutions like Equation (22) are commonly taught. Not only is the solution of Equation (20) more elegant and faster to evaluate than numerical integration, but its explicit form can serve as a basis for further analytical manipulations and derivations to analyse particular problems. Illustrating this point, the theory of galaxies has benefited from Freeman’s analytic solution for the circular velocity of exponential disks [28]. This velocity can also be computed by direct numerical integration, but the explicit expression in terms of Bessel functions has greatly simplified further studies.

The explicit solution also offers insights pertaining to symmetry properties (Sections IV C and IV D) and a connection between spherical collapse motions and probability theory. Finally, Equation (20) can serve as an exact benchmark for testing numerical integration techniques and simulation codes, e.g., for hydrodynamic and gravitational simulations.

An avenue for research in pure mathematics is an extension to complex-valued functions $r(t)$, where additional symmetries in the complex plane exist for $\gamma \in \mathbb{N}$.

ACKNOWLEDGMENTS

I thank Dr. Martin Bruderer, Dr. Aaron Ludlow, Dr. Zachari Slepian, Dr. Dmitry Sinelshchikov and Prof. Stefani Mancas for insightful suggestions that have inspired and improved this work. I am also grateful to Dr. Roberto Iacono for bringing to my attention the convenience of using the regularised incomplete beta function in transitioning from Equation (15) to Equation (20a), bypassing an earlier method invoking the hypergeometric function. I also acknowledge an anonymous referee of an earlier draft, for pointing me toward the substitutions discussed in Section ?? . Last but not least, I extend my gratitude to Dr. Mohamed Farhat and Prof. Andrea Prosperetti for many past discussions, which were a source of inspiration in writing this paper. I am a recipient of an Australian Research Council Future Fellowship (FT190100083) funded by the Australian Government.

Appendix A: Analytical derivation

Equation (8a) can be rewritten to separate time from position coordinates,

$$dt^2 = \frac{1 + \gamma}{2(1 - r^{1+\gamma})} dr^2, \quad (\text{A1})$$

During the collapse ($0 < r < 1$), the RHS is positive for any $\gamma \neq -1$. Since the collapse is characterised by a

shrinking radius ($dr < 0$) with growing time ($dt > 0$), we are interested in the negative branch,

$$dt = - \left[\frac{1 + \gamma}{2(1 - r^{1+\gamma})} \right]^{1/2} dr. \quad (\text{A2})$$

Let us integrate this equation backward in time from the dimensionless collapse time τ to an earlier time $t > 0$,

$$\int_{\tau}^t dt = - \left[\frac{|1 + \gamma|}{2} \right]^{1/2} \int_0^{r(t)} \frac{dr}{|1 - r^{1+\gamma}|^{1/2}}. \quad (\text{A3})$$

The lower bound of the second integral is zero by definition of the collapse time. To simplify the notation of the following equations let us introduce the positive constant

$$\eta = \frac{1}{|1 + \gamma|}, \quad (\text{A4})$$

and let $s := r^{|1+\gamma|} \in [0, 1]$. With these substitutions, $r = s^{\eta}$ and $dr = \eta s^{\eta-1} ds$, and hence

$$\int_{\tau}^t dt = -\sqrt{\frac{\eta}{2}} \int_0^{s(t)} \frac{s^{\eta-1} ds}{|1 - s^{\pm 1}|^{1/2}}, \quad (\text{A5})$$

where the sign of the exponent in the denominator is equal to the sign of $1 + \gamma$. If this sign is negative, we multiply the numerator and denominator of the fraction by $s^{1/2}$. Then,

$$\int_{\tau}^t dt = -\sqrt{\frac{\eta}{2}} \int_0^{s(t)} \frac{s^{\alpha-1} ds}{(1 - s)^{1/2}}, \quad (\text{A6})$$

with $\alpha = \eta$, if $\gamma > -1$, and $\alpha = \eta + \frac{1}{2}$, if $\gamma < -1$. We can readily unify these two cases in the single equation

$$\alpha = \frac{1}{4} + \frac{3 - \gamma}{4|1 + \gamma|}. \quad (\text{A7})$$

We have defined α in this way to make the right-hand integral of Equation (A6) identical to the definition of the *incomplete beta function*, $B(x; \alpha, \beta) = \int_0^x y^{\alpha-1} (1 - y)^{\beta-1} dy$. Hence, Equation (A6) solves to Equation (15).

Appendix B: Code examples

The quantile function $Q(x; \alpha, \beta)$, which forms the heart of the explicit Equation (20a), is readily accessible in most programming languages: `qbeta` in R, `scipy.stats.beta.ppf` in PYTHON, `BETA.INV` in EXCEL, `InverseBetaRegularized` in MATHEMATICA, `InvIncompleteBeta` in the ALGLIB library for C++, C#, JAVA, PYTHON, DELPHI; etc. For reference, this section provides a few explicit code examples for plotting the collapse functions shown in Figure 2.

1. Gravitational collapse

The gravitational collapse of a uniform pressure-free sphere is governed by Equation (7). The solution $r(t)$ in natural units R_0 and $T_0 = \sqrt{R_0^3/(GM)}$ is given by Equation (20a) with $\gamma = -2$. Perhaps the most compact implementation is achieved in the statistical language R, where three lines suffice to evaluate and plot this explicit solution:

```
tau = beta(3/2,1/2)/sqrt(2)
r = function(x) qbeta(1-x/tau, 3/2,1/2)
curve(r,0,tau,1000)
```

The resulting plot is analogous to the yellow line for $\gamma = -2$ in Figure 2. Most astrophysicists might be more accustomed to PYTHON, where this code could read:

```
import numpy as np
import matplotlib.pyplot as plt
from scipy.stats import beta
from scipy.special import beta as betafct

tau = betafct(3/2, 1/2)/np.sqrt(2)
def r(t):
    return beta.ppf(1-t/tau, 3/2, 1/2)

tvalues = np.linspace(0, tau, 1000)
plt.plot(tvalues, r(tvalues))
plt.show()
```

2. Cavitation bubble collapse

Readers closer to cavitation dynamics than astrophysics may consider the example of a spherical cavity collapsing in an incompressible liquid of density ρ , without viscosity and surface tension. Assuming a constant driving pressure Δp , the bubble evolution is governed by Equation (10); hence the collapse motion $r(t)$ in natural units R_0 and $T_0 = R_0 \sqrt{\rho/\Delta p}$ is given by Equation (20a) with $\gamma = -4$. The corresponding R script reads:

```
tau = beta(5/6,1/2)/sqrt(6)
r = function(x) qbeta(1-x/tau, 5/6,1/2)^(1/3)
curve(r,0,tau,1000)
```

This code reproduces the red line for $\gamma = -4$ in Figure 2. In PYTHON, this could be implemented as:

```
import numpy as np
import matplotlib.pyplot as plt
from scipy.stats import beta
from scipy.special import beta as betafct

tau = betafct(5/6, 1/2)/np.sqrt(6)
def r(t):
    return beta.ppf(1-t/tau, 5/6, 1/2)**(1/3)

tvalues = np.linspace(0, tau, 1000)
plt.plot(tvalues, r(tvalues))
plt.show()
```

-
- [1] J. E. Gunn and I. Gott, J. Richard, On the Infall of Matter Into Clusters of Galaxies and Some Effects on Their Evolution, *Astrophys. J.* **176**, 1 (1972).
- [2] C. C. Lin, L. Mestel, and F. H. Shu, The Gravitational Collapse of a Uniform Spheroid., *Astrophys. J.* **142**, 1431 (1965).
- [3] Z. Slepian and O. H. E. Philcox, A uniform spherical goat (problem): explicit solution for homologous collapse's radial evolution in time, *Monthly Notices of the Royal Astronomical Society: Letters* **522**, L42 (2023).
- [4] S. K. Foong, From moon-fall to motions under inverse square laws, *European Journal of Physics* **29**, 987 (2008).
- [5] G. Stokes, Notebook preserved in the Cambridge University Library, Add. MS. 7656. NB23. (1847).
- [6] L. Rayleigh, On the pressure developed in a liquid during the collapse of a spherical cavity, *Phil. Mag.* **34**, 94 (1917).
- [7] D. Obreschkow, M. Bruderer, and M. Farhat, Analytical approximations for the collapse of an empty spherical bubble, *Phys. Rev. E* **85**, 066303 (2012).
- [8] P. Amore and F. M. Fernández, Mathematical analysis of recent analytical approximations to the collapse of an empty spherical bubble, *The Journal of Chemical Physics* **138**, 084511 (2013).
- [9] N. A. Kudryashov and D. I. Sinelshchikov, Analytical solutions of the rayleigh equation for empty and gas-filled bubble, *Journal of Physics A: Mathematical and Theoretical* **47**, 405202 (2014).
- [10] N. A. Kudryashov and D. I. Sinelshchikov, Analytical solutions for problems of bubble dynamics, *Physics Letters A* **379**, 798 (2015).
- [11] H. J. Lane, On the theoretical temperature of the Sun, under the hypothesis of a gaseous mass maintaining its volume by its internal heat, and depending on the laws of gases as known to terrestrial experiment, *American Journal of Science* **50**, 57 (1870).
- [12] R. Emden, *Gaskugeln* (Leipzig: B. G. Teubner, 1907).
- [13] E. R. Harrison and R. G. Lake, Polytropic and Isothermal Plane-Symmetric Configurations, *Astrophys. J.* **171**, 323 (1972).
- [14] A. R. Klotz, Bubble dynamics in N dimensions, *Physics of Fluids* **25**, 082109 (2013).
- [15] G. Duffing, *Erzwungene Schwingungen bei veränderlicher Eigenfrequenz und ihre technische Bedeutung*, Series: Sammlung Vieweg No. 41-42 (Vieweg & Sohn, 1918).
- [16] A. H. Salas, J. E. Castillo Hernández, and L. J. Martínez Hernández, The duffing oscillator equation and its applications in physics, *Mathematical Problems in Engineering* **2021**, <https://doi.org/10.1155/2021/9994967> (2021).
- [17] S. C. Mancas and H. C. Rosu, Evolution of spherical cavitation bubbles: Parametric and closed-form solutions, *Physics of Fluids* **28**, 10.1063/1.4942237 (2016).
- [18] D. Obreschkow, M. Tinguely, D. Nicolas, K. Philippe, de Bosset Aurele, and F. Mohamed, The quest for the most spherical bubble: experimental setup and data overview, *Experiments in Fluids* **54**, 10.1007/s00348-013-1503-9 (2013).
- [19] J. R. Oppenheimer and H. Snyder, On Continued Gravitational Contraction, *Physical Review* **56**, 455 (1939).
- [20] F. Mirabel, The formation of stellar black holes, *New Astronomy Reviews* **78**, 1 (2017).
- [21] A. Loeb and F. A. Rasio, Collapse of Primordial Gas Clouds and the Formation of Quasar Black Holes, *Astrophys. J.* **432**, 52 (1994).
- [22] S. Aarseth, *Gravitational N-Body Simulations: Tools and Algorithms*, Cambridge Monographs on Mathematical Physics (Cambridge University Press, 2009).
- [23] P. Girichidis, L. Konstandin, A. P. Whitworth, and R. S. Klessen, On the evolution of the density probability density function in strongly self-gravitating systems, *The Astrophysical Journal* **781**, 91 (2014).
- [24] M. Farhat, What we learned from cavitation bubbles in microgravity, in *Preparation of Space Experiments*, edited by V. Pletser (IntechOpen, Rijeka, 2020) Chap. 5.
- [25] G. Rousseaux and S. C. Mancas, Visco-elastic cosmology for a sparkling universe?, *General Relativity and Gravitation* **52**, 10.1007/s10714-020-02705-y (2020).
- [26] H. C. Rosu, S. C. Mancas, and C.-C. Hsieh, Superfluid Rayleigh-Plesset extension of FLRW cosmology, *Annals of Physics* **429**, 168490 (2021).
- [27] M. N. Shneider and M. Pekker, Cavitation model of the inflationary stage of big bang, *Physics of Fluids* **33**, 017116 (2021).
- [28] K. C. Freeman, On the Disks of Spiral and S0 Galaxies, *Astrophys. J.* **160**, 811 (1970).